

Article

Surface Geomorphological Features of Deep-Seated Gravitational Slope Deformations: A Look to the Role of Lithostructure (N Apennines, Italy)

Guido S. Mariani ^{1,*}  and Andrea Zerboni ² 

¹ Dipartimento di Scienze Chimiche e Geologiche, Università Degli Studi di Cagliari, Cittadella Universitaria (Blocco A), 09042 Monserrato CA, Italy

² Dipartimento di Scienze Della Terra 'A. Desio', Università Degli Studi di Milano, Via L. Mangiagalli 34, 20133 Milano MI, Italy; andrea.zerboni@unimi.it

* Correspondence: guidos.mariani@unica.it

Received: 30 June 2020; Accepted: 21 August 2020; Published: 22 August 2020



Abstract: The attention to deep-seated gravitational slope deformations (DSGSDs) has steadily increased in the last few decades, because such features are ubiquitous in mountain areas. Their geomorphological surface expression, especially when related to the effects of lithostructural control in sedimentary stratified bedrocks, is well characterized in theory, but sometimes not as well documented in field cases. In this contribution the investigation of several DSGSDs in the area of the Northern Apennines of Italy is reported. A survey of the area was conducted using fast and low-cost satellite imaging techniques, in order to describe the surface features of selected DSGSDs and verify how their occurrence is linked to the effect of lithostructural constrains such as bedding and folding. Surface features developed in parallel to the strike of the slope are mostly related to the main gravitative strain acting on the deformation. Features along slope dip are instead formed by the release of tension caused by compressive forces at the landslide foot or by the presence of pre-existing weak lines. One example of a DSGSD, formed on the hinge of a vertical fold, shows a corrugated appearance due to the release of vertical fractures that mask most other features usually associated with DSGSDs. This potentially impairs the detection of these landforms during field and remote surveys.

Keywords: deep-seated gravitational slope deformations; mountain geomorphology; lithostructure; slope stability; Apennines

1. Introduction

In the last few decades, deep-seated gravitational slope deformations (DSGSDs) have been established as one of the common geomorphological features of the world's mountain landscapes [1,2]. Since the first studies on these landforms [3–6], their presence has now been reported for many mountain chains, with numerous examples from across continents [6–23] and even from other planets [24–26]. In these decades, the interest towards the origin and the evolution of these landforms has attracted an increasingly wide amount of studies.

A major portion of the scientific effort was, and still is, aimed to identify major DSGSDs, their relevance in terms of representing potential geohazards, and to uncover the causes of their formation and their subsequent dynamics. Many structural models have been postulated to interpret the processes responsible for the detachment of such large slope landforms and the conditions that enable their movement, dormancy, and possible reactivation [18,20,27,28]. The origin itself of these landforms is still a matter to be settled completely. DSGSDs have in time been associated

with the action of tectonic stress [18,29–31], seismicity [6,14,32,33], groundwater regime and karst processes [20,27,29,34,35], glacial rebound [36–39], lithology and bedding [18,27,40,41]—usually in combination with each other. The complex interactions between these factors strongly influence further development and behaviour of DSGSDs, which often undergo cycles of dormancy and reactivation. In tectonically active landscapes, the structural control likely plays a central role in triggering successive movement phases [16,30]. The role of pre-existing fault systems in most cases is a fundamental primer both for the initial detachment and the further movement of DSGSDs [42–44]. In this light, seismicity or post-glacial unloading, often claimed as reactivation controls, can also serve as triggering factors for new DSGSDs [2,32,38,45,46]. This goes hand in hand with the movement dynamics of these landforms, where the action of time-dependent creep rheology is often postulated as a major driver in the activation of a shear zone [27].

The exact knowledge of the processes driving the development of DSGSDs is clearly important. Do they form in sudden events or as the product of multiple spaced reactivations over short periods? Or is it a slow constant movement with no or negligible reactivations? Such questions have a sizable impact on landscapes and their inhabitants. In fact, the circumstances and potential consequences of the reactivation of these landforms are of high interest in view of the potential geomorphological risks it might imply for the human landscape. The possibility for catastrophic landslides started by sudden detachments is a subject on which research has concentrated for a long time, and DSGSDs are no exception [33,47–51]. Occasionally, human activity itself might become a relevant factor in the reactivation of these landforms [52,53].

The investigation of the surface morphology of DSGSDs is a vital step in the description and interpretation of their evolution. This approach can potentially bring new useful diagnostic tools for the first and fast detection in the landscape, and allow to characterize them from both field and remote sensing observations. For this purpose, it is essential to gain precise knowledge of the different types of surface expression of DSGSDs and then correlate the surface features to specific conditions that produced the slope deformation events. In this way, it would be possible to give accurate preliminary estimates of the distribution and characteristics of these landforms on the territory, with obvious implications in terms of landslide risk assessment and monitoring of the wider landscape. Many structural elements such as faulting have been thoroughly investigated and are well known in the literature [14,18,31,54]. The lithostructural control on geomorphological features, such as the effect of bedding and folding of geological strata, is also known in terms of influence on DSGSD development since the classification of Varnes [55] and widely investigated [41,51,54,56–59]. Comparisons between different lithostructural settings for DSGSDs are known well as models, but field examples are not as easy to find, especially once considering the effect of stratification. When taken into account in a theoretical setting, sedimentary strata are often considered together with metamorphic foliations [27]. As a result, though previous studies did show how stratification and folding were critical in driving the behaviour of the structural features at the DSGSD surface [41,56,57,60–63], sedimentary structures were sometimes underrepresented in practice as a contributing factor in the development of DSGSDs.

In this work, a local study concerning the expression of geomorphological surface features of different DSGSDs developed on sedimentary successions is reported. The aim is to describe and classify, from a remote observational point of view, the surface morphology of DSGSDs in order to provide examples of the influence of folds and bedding and the role played by lithostructural control on DSGSD development. In order to achieve this, this study surveyed and compared several DSGSDs developed on different geological conditions in the northern Apennines of Italy (Figure 1). These results confirm how lithostructural settings play a prominent role in the evolution of the surface features of DSGSDs, independently from the triggering factor. Moreover, the use of open-source data and software makes such method reliable. Finally, the methods used in this study can be applied in the absence of high-resolution survey technologies, namely LiDAR (light detection and ranging) data, still poorly available for many areas in the world, as well as in remote, inaccessible regions.

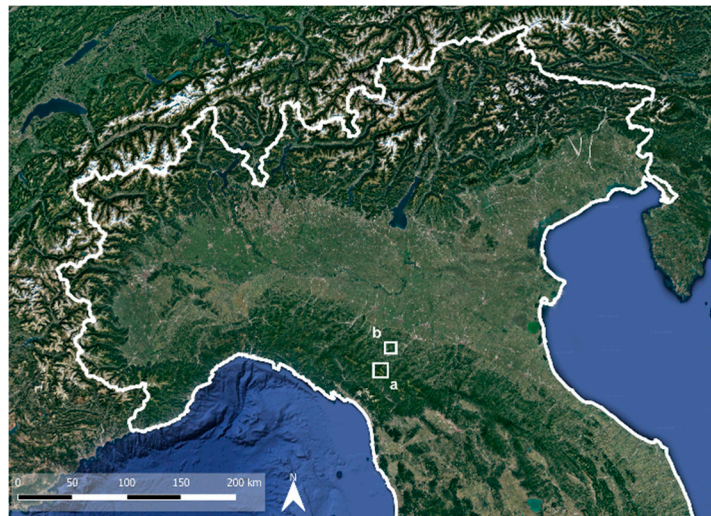


Figure 1. Google Earth™ satellite image (Landsat/Copernicus 2020, seen on 30 July 2020) showing the location and general setting of the study areas: (a) Ozola River valley area; (b) Carpineti ridge area.

2. The Study Area

The outer arc of the northern Apennines inside the Emilia-Romagna region in northern Italy is famous for the high complexity of its landscape. This is mostly derived from its lithostructural setting, which is responsible for the development of most slopes. The landscape shows a wide variety of structural and slope landforms, among which many DSGSDs are already known and surveyed [64]. At the same time, the geology of this area bears an overall similarity in its lithologies and orogenetic development, which is useful in being able to directly compare landforms located at substantial distances from each other (tens of kilometres).

The northern portion of the Italian Apennines is an orogenic arc verging NNE, in which sedimentary units have been heavily deformed. Deformation both preceded and drove the formation of the chain, affecting deposits formed during the Mesozoic and Cenozoic [65,66]; the chain also includes ophiolitic elements dislocated by compressive uplift. The inner arc of the chain is complex and characterized by extensional tectonics [65]. The outer arc is a regular succession of outward-migrating deformational belts, characterized by widespread folds and thrusts following the direction of the deformation [67,68], thus resulting in widely distributed fault systems. The stratigraphy of the northern Apennines follows a classic series of siliciclastic turbidite foredeep wedges [69,70], widely deformed in a series of folds and overthrusts in the inner portion of the chain. Lithologically, this results in widespread, outcropping turbiditic formations, especially in the higher part of the chain. Marls and limestone formations are also common [71]. The high degree of deformation induced intense faulting and fracturing throughout all these formations and lithologies.

Structural deformations provide a strong control on surface landforms and influence the geomorphological evolution of the northern Apennines. In this mountain environment, folds and thrusts visibly occupy the elevated points and ridges, forming cuesta-type and occasionally tabular reliefs, which characterize the entire area [65,72]. The most important structural ridge systems follow the alignment of the chain NW to SE, according to the axis of the main folds [71], but many other smaller elements can be found scattered or isolated. Current and recent tectonic activity, and the associated mechanical features of the substrate, relate to the widespread frequency of slope movements in the area. Landslides are a characteristic feature of the landscape of the northern Apennines [73] and have been widely investigated and monitored in the last few decades [74], with several tens of thousands of large mass movements and complex landslides inventoried [75]. Especially large landslides can be reported, often in direct relation to faulting and neotectonics [76]. Landslides of different nature and extension deeply affected the territory in the past in response to climate variations [77], with clear phases of slope instability detected during the Holocene [78,79]. Phases of slope instability and

landslide reactivation are recorded even for the present time [80,81]. Erosional landforms induced by water action are widespread: lithologies have a strong influence on these processes, with jagged cliffs and gorges on sandstone and limestone, and hummocky hill landscapes strewn by occasional Badlands on claystones [22,82]. The highest parts of the Apennines were modelled by glaciers during the last glacial periods [83], before their physical disappearance at the end of the Pleistocene [84]. The impact of glaciers is still visible on the landscape, particularly in the form of till deposits [22]. In this context, the potential for the development of DSGSD is very high, and consequently attention to this topic has increased in the area in recent years [33], as well as for the rest of the Apennines in general [13].

Two main landmarks of the Apennine landscape were chosen for this study (Figure 1). The Ozola River valley and its surrounding areas represent a high mountain environment with high peaks and steep slopes, located close to the main watershed of the Apennines. Elevations span between 900 to 2000 m a.s.l., with several noteworthy peaks and structural ridges. The Carpineti ridge is located in an intermediate position between the highest peaks to the southwest and the Po plain to the northeast, with elevations contained between 300 to 900 m (mid-altitudes for the Apennine chain). It is a long and continuous structural cuesta extending SW to NE for almost 10 km, with the cataclinal slope facing NW and the anaclinal slope facing SE.

3. Materials and Methods

The geomorphological investigation of DSGSDs took place mainly through remote sensing, with the acquisition and processing of topographical, geological, satellite, and drone data, and the construction of interpretative models. These data and interpretative models were then verified in the field. The most recent studies tend to use LiDAR data, freely available from many institutions [33,51,85]. Unfortunately, this is not always a viable method: in many areas of the world, such as our region of interest, LiDAR data are still not available or are scattered and discontinuous, and do not provide full or adequate coverage of the investigated landforms. While the collection of high-resolution data in the field has been made easier by the newer advances in technology and the availability of affordable equipment, field accessibility can be problematic in many situations around the world. For instance, the reduced mobility imposed by abrupt events such as the Covid19 pandemic promotes the necessity to adopt remote investigation technologies. Consequently, in order to emphasize data accessibility, this study uses middle-resolution non-LiDAR digital terrain models (DTM) as the base for remote sensing. Field control was carried out only by checking the nature and geomorphological characteristics of the surface features recognized in remote sensing (Figure 2). Further verification through a high-resolution LiDAR survey can also be completed in the future.

Open source data from multiple archives were acquired. Official digital 1:5,000 scale topographical mapping [86] reprojected to the UTM reference system, zone 32N, provided the topographical layers of the map used for the preliminary identification of the landforms, together with aerial photos [86]. GoogleEarth™ high-resolution satellite images provided additional information to aid visualization and survey planning. As the basis for digital analysis, a 5 m resolution digital terrain model (DTM) was retrieved online from the Geological Survey of the Emilia-Romagna region [86], and reprojected to the UTM reference system, zone 32N. QGIS software tools (version 3.4, www.qgis.org) were used to build slope, aspect and hill shade models to support visualization and analysis of the landforms. Using the *QGIS 3D map view* tool and the *Qgis2threejs* plugin, a topographic model for each identified DSGSD (see below) and its surrounding landscape was made from the DTM. Geological information on the area, including lithological and structural features (i.e., nature of bedding), along with data on Quaternary surface deposits were integrated using 1:10,000 scale geological maps provided by the Emilia-Romagna region Geological Survey [87]. These data were reprojected to the UTM reference system, zone 32N, and combined with the DTM in order to observe the general 3D setting of the strata.

For the two sample areas chosen, DSGSDs were identified and outlined by visual observation. From this inventory, four different DSGSDs were chosen to investigate in detail. For each DSGSD all visible surface landforms were mapped from the model, and from the combination of slope, aspect and

hill shade layers. Each landform was then catalogued and interpreted according to its appearance with the support of the geological data. Considering the descriptive purpose of this work, it was decided not to conduct morphometric analysis on the landforms and focus instead on their occurrence and general arrangement. Fieldwork was conducted after the elaboration and interpretation of digital data and focused on the verification of the landforms recognized and described in remote sensing.

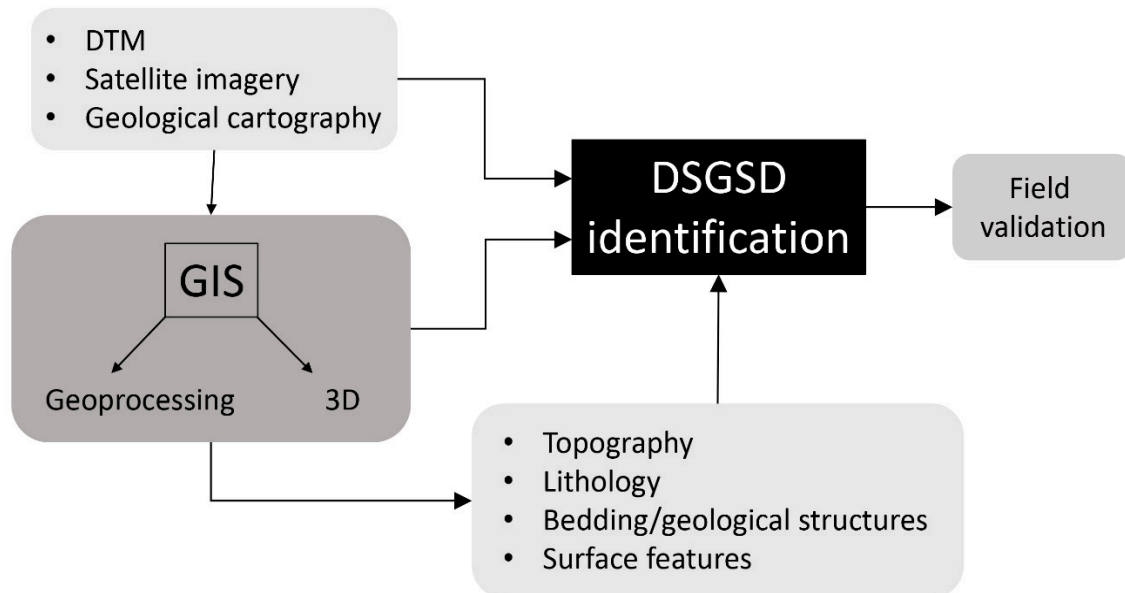


Figure 2. Workflow of the methodology used in the investigation of deep-seated gravitational slope deformations (DSGSDs) in this study.

4. Results

The two studied areas show differences in the number and dimensions of the DSGSDs recognizable in remote sensing due to their differences in topography and structural elements. The Ozola River valley is located in the highest portion of the chain; the ridge of its southern slope is the main Apennine watershed. Here, slopes are higher (up to 1100 m) and thrust faults and fault systems are widespread. This area shows a high number of large and sometimes complex DSGSDs (Figure 3a). Other areas display DSGSDs that are barely visible on the topography, sometimes only detectable by the thin border of the landform itself. The Carpineti ridge shows two different slope settings: its southern slope is steeper, forming a clear escarpment. The northern one follows a lower slope angle; it is cut by parallel streams, which form a series of v-shaped incisions downwards along the slope. Compared to the previous area, here slopes tend to be smaller in height (no more than 600 m high) and faulting is relevant but more irregularly distributed. DSGSDs are sparser in number (Figure 3b) and their average dimensions are smaller. In both areas, the distribution of DSGSDs is clearly influenced by structural elements. Most of them are located on the slopes of the main structural landforms, particularly on the northern sides of the Ozola valley and of the Carpineti ridge. The close presence of fault systems is also a common feature in the two areas.

Four DSGSDs were chosen taking into account both topographical and lithostructural criteria. In particular, the overall dimensions and the diversity of visible surface features were the considered factors as well as the overall structural setting. Multiple or multidirectional folding that would have made interpretations and models particularly challenging were avoided. The four chosen DSGSDs show an array of different surface features, which can be described in detail. Firstly, the main topographical features of the area are described, examining the position of the deformation in the wider landscape through its elevation, aspect and slope values. Secondly, an assessment of the geological setting of each DSGSD and adjacent areas is made, taking into account the lithologies composing the bedrock and all the available information on bedding and structural features, in particular folding and faulting. Finally,

a detailed description of the geomorphological surface features found on each landform is made listing all the types present, together with their characterisation in qualitative terms (Table 1). While the general scale of these landforms is several hundreds of meters smaller than the usual examples found in literature, they all show the diagnostic features outlined by Jaboyedoff et al. [88]. They are also related to fault systems and major structural features, which likely control their evolution.

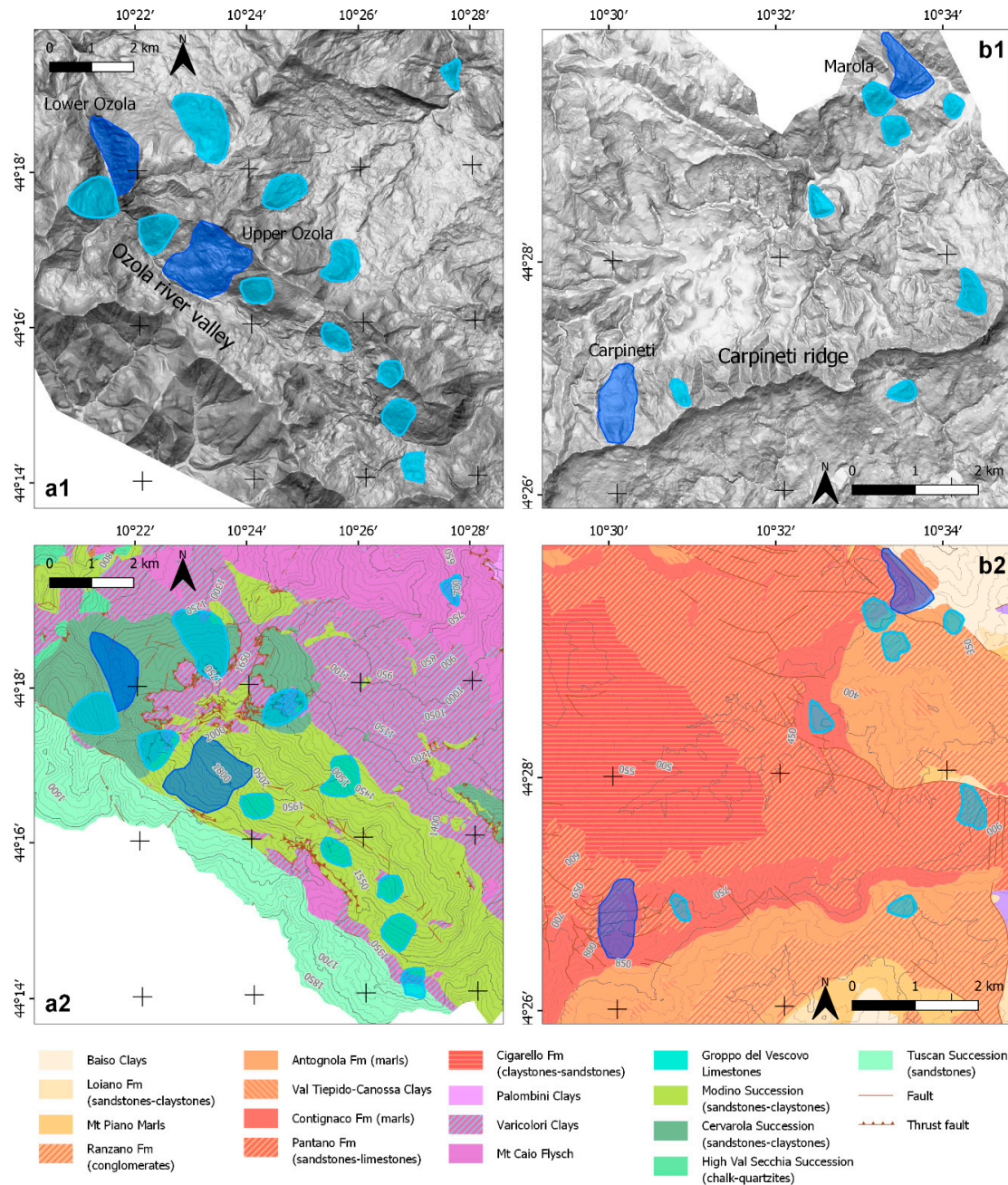


Figure 3. Inventory of the identified DSGSDs for the Ozola river valley and Carpineti ridge study areas. DSGSDs are shown in light blue, whilst those landforms investigated in detail are in blue. In (a1) and (b1), the background is the hill shade model produced from the digital terrain model (DTM) [86], in (a2) and (b2) the geological map at scale 1:50,000 [87].

4.1. The Upper Ozola DSGSD

The Upper Ozola DSGSD is a very large deformation on the northern slope of the Ozola river valley and developing in height from its crest (2000 m a.s.l.) to the bottom of the valley (1300 m a.s.l.), with an average steepness of 20° (Figure 4a). The bedrock is the same for the whole DSGSD: the Mt. Modino sandstone [89], composed of coarse-grained turbiditic deposits. In the area of the DSGSD, strata dip to the NE with bedding between c. 20° and 50°, forming an anaclinal slope with the valley. A main fault, visible to the W, cuts the slope transversally in a W–E direction and is highlighted by a fracture on the surface of the gravitational deformation itself.

The deformation is wide and divided into three different bodies. The two smaller ones lie at the top of the slope, at the sides of the main deformation. They are outlined at the ridge of the slope by a definite scarp edge, which shows several double crests along the eastern body and a very clear ridge top depression on the western one. Counterscarps and trenches are visible on both (Figure 5a); the eastern one also presents the initial formation of a toe in its lower section. The main body of the DSGSD occupies most of the height of the slope. Just below its top is a flatter area (about 10–15°) that hosts a sequence of counterscarps and trenches that are sometimes discontinuous. Downslope, the slope bulges forward forming multiple toe-thrusts features overlying each other at different heights. Several surface landslide detachments also appear. Other features often observed at the bottom of DSGSDs [44,85], such as vertical cracking and tension failures, are not visible. Between the trench system and the bulge below, a smooth area is present. Here a noticeable fracture forms a shallow and straight E–W striking valley which cuts into the main body of the landslide, following precisely the direction of the fault noted above, immediately west of the DSGSD.

Table 1. Surface geomorphological features identified on each investigated DSGSD.

DSGSD	Lithostructure	Strike-Parallel	Surface Features Dip-Parallel	Complex
Low Ozola	Fold hinge	Counterscarp scarp edge	Vertical fractures	Toe bulge
High Ozola	Anaclinal slope	Counterscarp double crest landslide edge landslide scar ridge top depression scarp head trench	Tension cracks	Toe bulge Unloading valley
Carpineti	Cataclinal slope	Counterscarp landslide scar ridge top depression trench		Unloading valley
Marola	Anaclinal slope	Unloading valley landslide scar landslide edge ridge top depression	Tension cracks	Toe bulge

4.2. The Lower Ozola DSGSD

Downslope from the Upper Ozola DSGSD, 1.5 km to the NW, the valley changes direction after a bend in the path of the Ozola stream from NW to NNW (Figure 4b). Here the Lower Ozola DSGSD occupies the whole height of the eastern slope from top (1600 m a.s.l.) to bottom (800 m a.s.l.). Like the former, this DSGSD lies on a single rock formation: the Mt. Cervarola sandstone [89], another coarse-grained turbiditic succession. Bedding instead changes, because this location is occupied by an E–W oriented anticline. Therefore, strata dip at different angles along the deformation, roughly moving away from its main body. At the top of the DSGSD lies the fold axis and strata are almost flat,

dipping at a very low angle (around 5°) to the E. Other fault lines are scattered outside the deformation to the E (Figure 4b).

The nature and distribution of surface features on this landform diverge sensibly from the rest of the studied DSGSDs. The only common feature appears on the summit of the slope: here, a well-defined continuous detachment edge follows the entirety of the landform. Just below it, quite close to the edge, there is a single visible counterscarp, which is followed downwards by a sharp cliff some tens of meters high, with evidence of rock toppling processes. The rest of the landform shows more specific features: the body of the deformation is deeply cut by a series of parallel vertical cuts developed along elongated fractures running along the slope. Erosion seems to have further deepened the cuts, producing a continuous layer of talus deposits at the bottom of the slope. The shape of talus cones can still be recognized in the deposits at the bottom of each cut. No discernible toe is visible in the lower section of the DSGSD.

4.3. The Carpineti DSGSD

The Carpineti deformation lies on the northern slope of the larger morphostructure of the Carpineti ridge, bordered by two valleys (Figure 6a). It starts at the ridge crest (900 m a.s.l.) and follows the slope downwards to the North, bending NE towards the bottom (600 m a.s.l.) along the path of the valley below it. The lithology of the area varies between interbedded sandstones and claystones, and marls that belong to several rock formations (Pantano Fm., Contignaco Fm., and Antognola Fm. [89]). Strata follow the slope dipping northwards at various angles between 20° to 70° , forming a clear over-dip cataclinal slope. A clear system of parallel faults is present in the area of the DSGSD, with evidence at both of its sides (Figure 6a).

The DSGSD has the appearance of a single body, with a clear downslope oriented elongated shape. It consists of a series of counterscarps and trenches separating blocks of weakly deformed rock without visible signs of bulging or further fracturing. At least five of these blocks can be recognized (Figure 5b). The presence of trenches can be related to a system of faults parallel to the ridge, which covers a large area of the slope, with the deformation at its centre. At the top, a small ridge-top depression is present. Two unloading valleys border the landform, converging at the base, just in front of the deposits of two landslide detachments located.

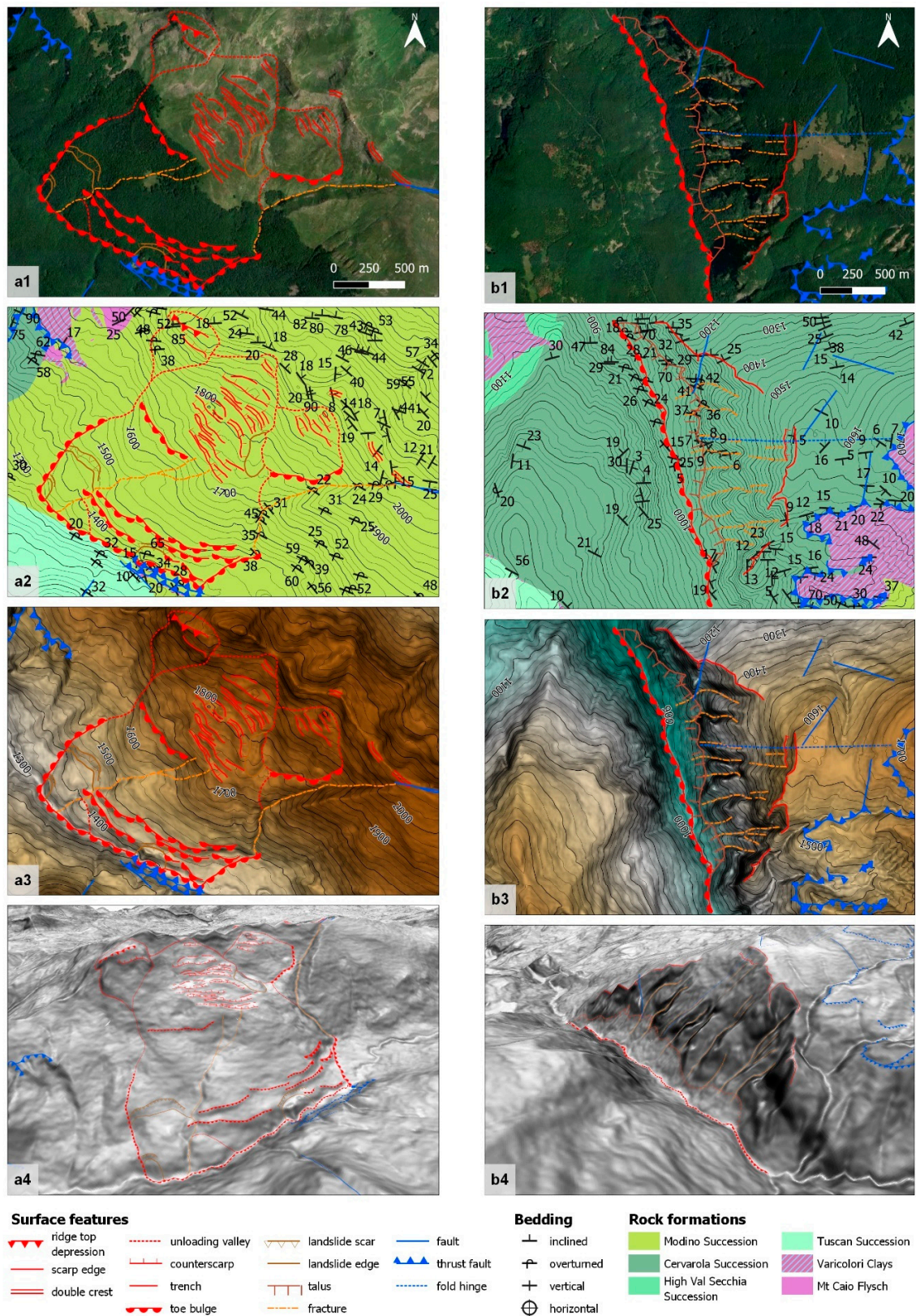


Figure 4. Detailed mapping of the DSGSDs in the Ozola River valley area: (a) Upper Ozola; (b) Lower Ozola. For both landforms the main surface geomorphological features are represented on: (1) Google Earth™ satellite image (Google 2020, seen on 30 July 2020); (2) geological map at scale 1:50,000 [87]; (3) colored DTM-slope layer mesh; (4) DTM-derived 3D model.

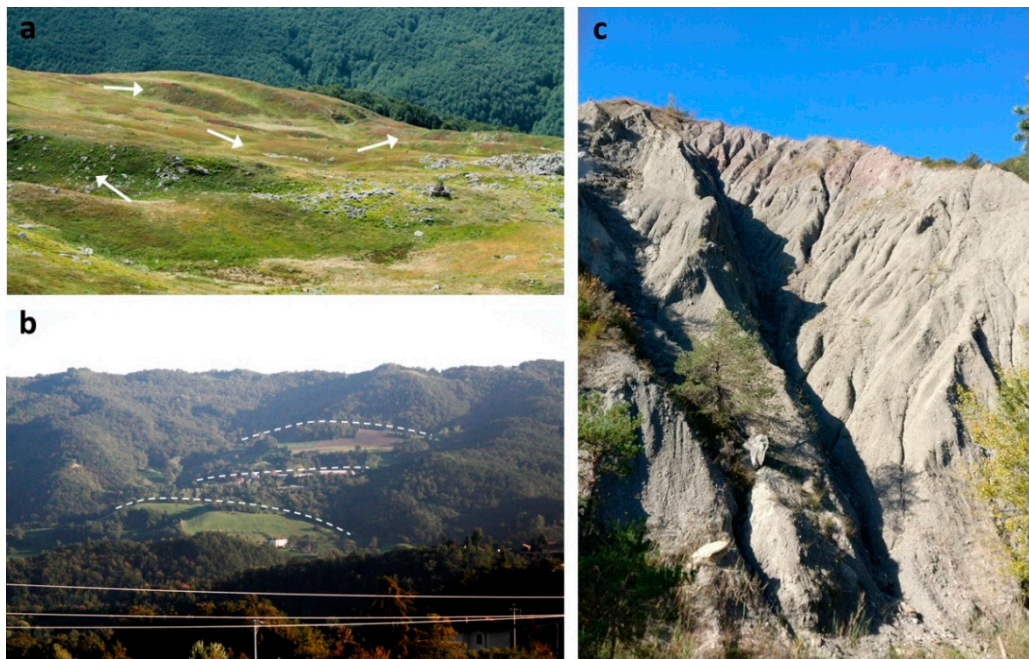


Figure 5. Selection of surface features on the studied DSGSDs: (a) counterscarps and trenches on the upper Ozola DSGSD (indicated by the arrows); (b) blocks of rocks separated by trenches and counterscarps on the Carpineti DSGSD (dashed lines); (c) vertical fractures on the main body of the Marola DSGSD; note the formation of badlands in the vicinity of fractures.

4.4. The Marola DSGSD

The Marola DSGSD is located approximately about 6 km NE from the Carpineti DSGSD, positioned on the NE slope of a lower NW–SE oriented small ridge, which abruptly ends southwards (Figure 6b). The deformation occupies the NE slope of the ridge and its SE side, with its highest point at the angle between the two slopes just below the crest (600 m a.s.l.); its lowest point lies at the bottom of the valley (350 m a.s.l.). The NE slope ends at a straight stream cut into soft marls (Antognola Fm., Mt. Piano marls) and clays (Baiso clays, Val Tiepido–Canossa clays). The upper portion of the slope is occupied by the same interbedded sandstones and claystones found in the Carpineti DSGSD (Pantano Fm., Contignaco Fm.), dipping SW opposite to the slope. The SW slope of the ridge is shorter and connects to a small steep valley at a higher elevation related to a fault trending NW–SE (Figure 6b). This area hosts several other faults, one of which connects to the SW border of the deformation.

The landform comprises different detachments. To the sides of the main body of the deformation three smaller ones are found, with two located to the North and one to the South. The northernmost ones are lower in elevation than the others, but wider. On the other side of the DSGSD to the south, the third lateral detachment slopes into the SE valley; its height reaches the main body of the DSGSD, but it occupies a thinner portion of the slope compared to the other smaller deformations. All the smaller bodies show no visible surface features except for the toe bulging in the northern ones. The main body of the DSGSD occupies the area of the slope at the corner between the two valleys. Most of the surface features are located here. Two small ridge top depressions appear on the summit of the deformation and further downslope, probably indicating a further detachment. The bottom toe is much more pronounced to the SE than to the NE. Vertical cracks are present on both sides of the main body (Figure 6b). To the NE they are linear and following precisely the direction of the slope; they are placed at regular intervals and cut progressively longer and deeper inside the deformation towards its corner. To the SE they are clustered in a single area; cracks are quite short and irregular, and form an angle with the valley instead of lying perfectly perpendicular through the slope. The appearance of the latter seems more related to a local area of highly fractured rock than to the effect of the gravitational deformation. Several landslides are also visible on the main body and on the southern lateral detachment.

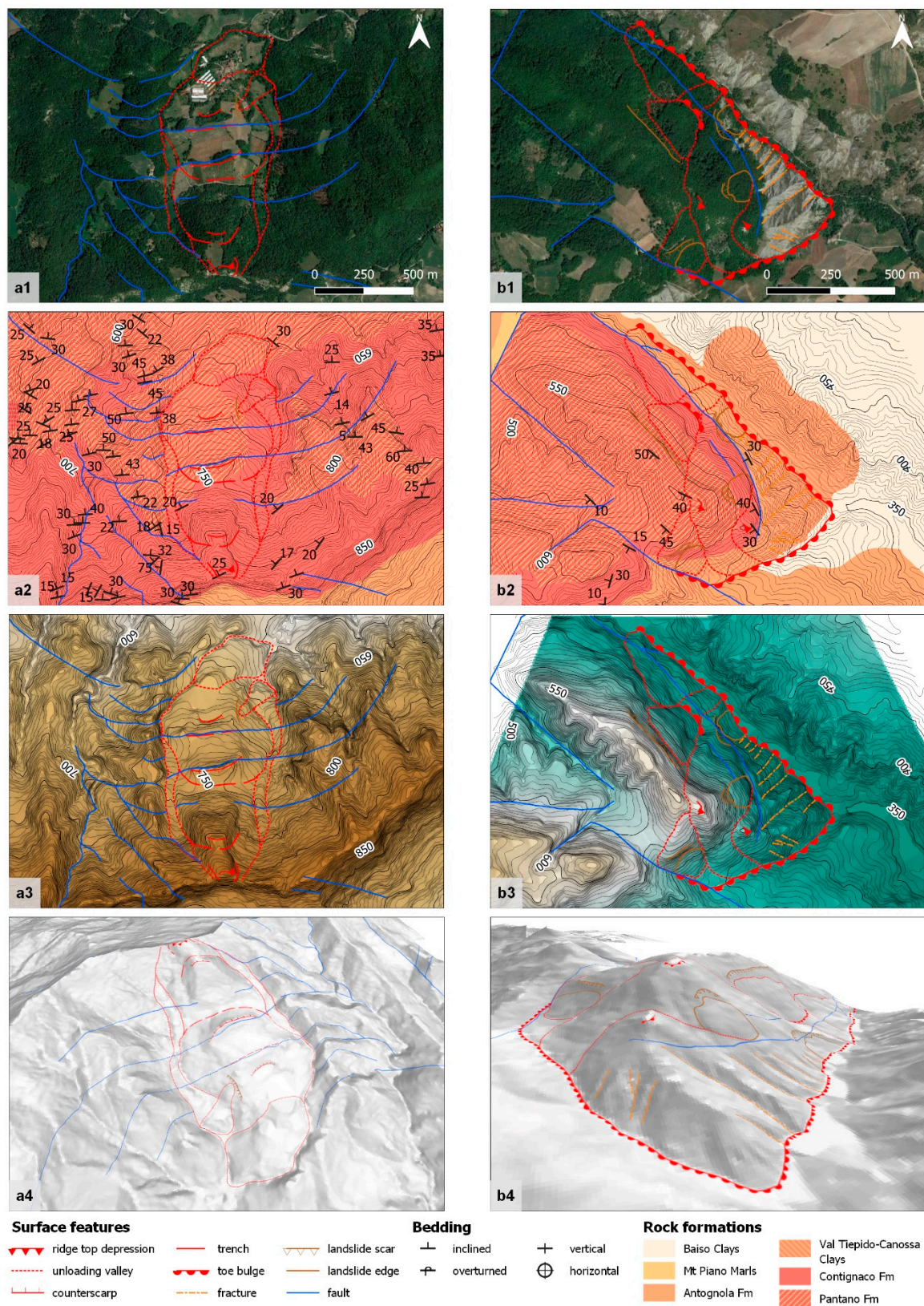


Figure 6. Detailed mapping of the DSGSDs in the Carpineti ridge area: (a) Carpineti; (b) Marola. For both landforms the main surface geomorphological features are represented on: (1) Google Earth™ satellite image (Google 2020, seen on 30 July 2020); (2) geological map at scale 1:50,000 [82]; (3) colorized DTM-slope layer mesh; (4) DTM-derived 3D model.

5. Discussion

5.1. Geometry and Development of Surface Features

From the surface evidence collected, it is possible to group the studied DSGSDs into different categories according to the typologies and frequency of their surface features. In aerial imagery, the effect of gravity on a sloping surface is the expression of the horizontal component of the gravitative stress, which approximately follows the dip of the slope. In particular, in a simplified DSGSD model the surface morphologies can be subdivided into two groups: (i) features formed by gravitational stresses which are roughly parallel to the slope strike and (ii) features generated by stress transversal to the slope that appear parallel to the slope dip and generally subvertical when observed from the front of the slope.

A large proportion of the surface features described for the studied DSGSDs can be attributed to the first group. A wide variety of features of this kind are present, including counterscarp and trench systems, double crests and ridge top depressions. Their development is related to the direction of the main stress, which follows the DSGSD downslope movement. Extensional forces applied to the body of the deformation seem to be the principal cause for the formation of this group of major visible features [12,31,44]. The other group of surface features is smaller and the most important is represented by the systems of parallel fractures cut along the slope formed by principal stresses that are perpendicular to the main direction of the DSGSD. Their positioning, the connection to the bottom part of the landform, and the regularity in their pattern link their formation to the release of tensile stress. This can be related to different causes, such as the presence of the gravitative compression caused by the downslope movement of the landform. Compressive forces induce vertical brittle structures in the rock and perhaps oblique movement, or even some internal re-activation of inherited structures during a progressive failure event. Tensile fractures on toe bulges are indeed formed in this way [43,88], though pre-existing weaknesses can produce the same features and form similar patterns. When fractures are not limited to the foot and instead affect the entire section of the landform, it is difficult to explain their genesis simply by the effect of bulging alone. Toe bulges often develop parallel to the fault strike but can adapt to topographical and structural constraints into less definable forms, making them quite complex features. The same can be said for unloading valleys, which should in theory follow the slope dip, but in practice are very variable and dependent from the pre-existing topography [88,90].

5.2. DSGSD Shape in Relation with Bedding and Folding

Considering the bedding characteristics for each of the studied DSGSDs, it can be seen how these affect the surface geomorphology of each landform in different ways. On the Carpineti deformation, located on a cataclinal slope, the main surface features belong to the first type of slope strike-parallel morphologies, more precisely trench and counterscarp systems and ridge-top depressions. On the DSGSDs of Upper Ozola and Marola, on anaclinal slopes, surface forms belong again to the first group, but with a greater complexity; toe bulges appear, as well as double crests, and in general surface morphologies are more diverse. Lower Ozola represents a special case, where strata belong to an anticline with a vertical axis transversally cut by the slope. Here, except for a couple of features attributable to the first group (a visible trench at the top of the landform and the main detachment scarp), the main surface forms are very pronounced vertical cuts (and related talus deposits) belonging to group two.

While representing only special bedding cases on which DSGSDs can appear [27], these examples are very representative of the different behaviour that stems from the different lithostructural setting of cataclinal and anaclinal slopes [56]. The case of Carpineti shows how the first ones amplify and help movement, producing a more expressed deformation in the longitudinal sense (Figure 7a) with packs of disjointed strata sliding over each other as successive shear zones. DSGSDs on cataclinal slopes might, in this sense, also imply a higher failure risk, with different blocks moving more independently between each other, as for example in the Carpineti DSGSD (Figure 6a). On the contrary, on anaclinal

slopes strata lie straight across the movement with a more modest influence on failure, and the DSGSD behaves differently. The result on the surface is a mixed presence of features from both groups, as the deformation causes the appearance of a larger variety of features (Figure 7b). This is visible in both the Upper Ozola (Figure 6a) and Marola (Figure 6b) deformations.

The completely different appearance of Lower Ozola, with its steep profile and parallel cuts, is most probably due to the presence of a completely different lithostructural setting. Here, the DSGSD is located on a fold axis with a horizontal or low-angle hinge line. In this particular case, the set of radial fractures (axial cleavage) associated with the structure (Figure 7d) appears at the surface as a series of close vertical fractures. The detachment of a DSGSD would probably activate these weaknesses and cause the opening of similarly oriented cuts at the surface. With the downslope progression of the DSGSD and the formation of a toe at the foot of the slope, further tension would be added to the fractures in the same way that tension cracks form on toe bulges. The help of surface processes such as water erosion would further deepen and exaggerate the appearance of these features. Following this hypothesis, it would be possible for these cuts to become the main surface features of the DSGSD over time, progressively forming a steeper slope and obliterating other surface features. The DSGSD would ultimately develop a corrugated appearance (Figure 7c,d), such as the one found on Lower Ozola, characterized by a series of parallel vertical ridges and cuts. Bedding in this case would not appear to have as significant an impact on the development of the landform as strata would not dip as steeply as the fractures and therefore would not develop as much. This is only one of the possible scenarios; many other combinations of cuts on differently shaped folds are possible in nature, each producing different configurations and surface features according to the relative influence of bedding.

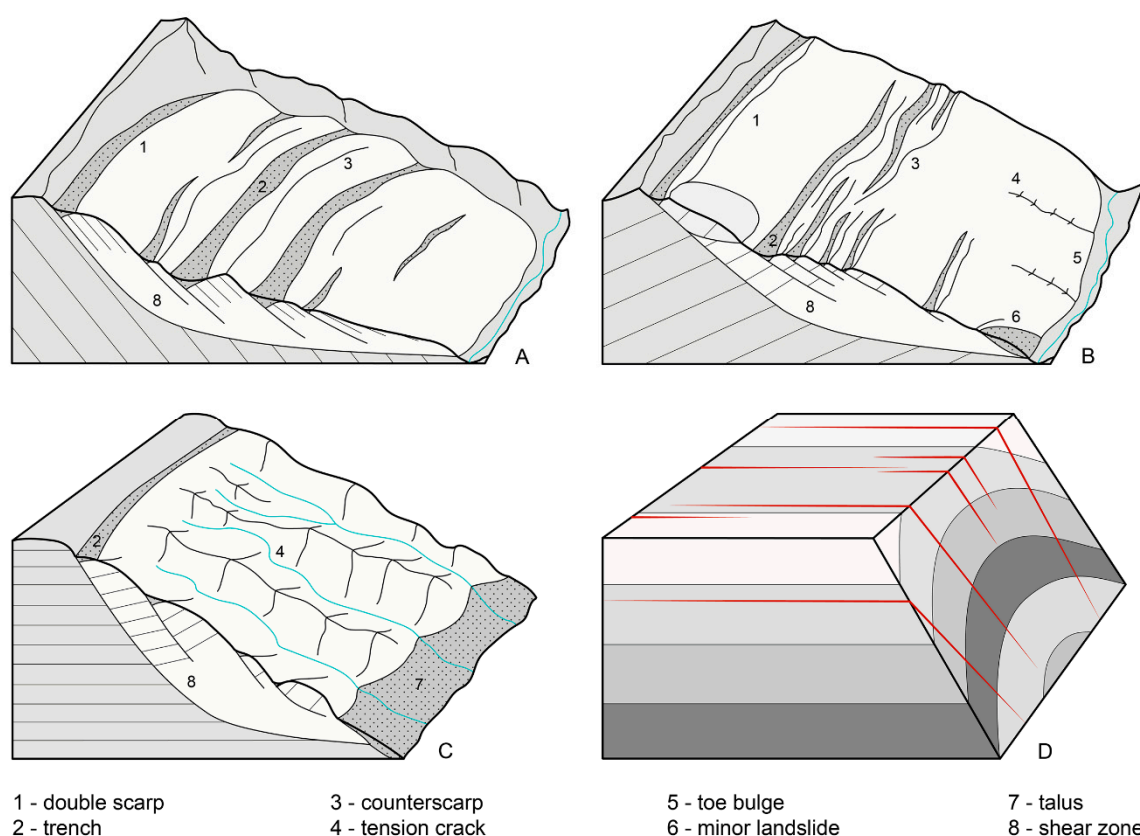


Figure 7. Theoretical models illustrating the development of surface geomorphological features of DSGSDs in relation to lithostructural settings: (A) DSGSD along a cataclinal slope; (B) DSGSD along an anaclinal slope; (C) DSGSD along horizontal strata at a fold hinge; (D) scheme of fractures associated with the fold hinge. The scale of the models is in the order of magnitude of the hundreds of metres.

A striking comparison can be made between the Upper and Lower Ozola DSGSDs. In fact, they share most of their geological setting and history; they belong to the same valley where they occupy the same slope at comparable elevations. Lithology is also mostly the same—sandstone, although referred to different formations (Mt. Modino Fm. and Mt. Cervarola Fm., respectively). As for their geomorphological history, the valley was interested by glacial advance and retreat during the Last Glacial Maximum, which is testified by the presence of valley steps [22]. These latter features allow to relate the evolution of both DSGSDs to glacial debuttressing as one trigger or reactivation factor, as it is commonly seen in case studies from other mountain ranges [37,38,44]. The only main difference between the two is the lithostructural setting in which these DSGSDs are developed. Their surface features can therefore be attributed to the influence of lithostructure, which in one case is represented by an anaclinal slope, in the other by a fold hinge. Vertical fracturing is not limited to this situation alone. For example, parallel fractures are present on the Marola deformation though bedding shows no evidence of folding in the immediate area. Fractures are instead probably triggered by stress release due to the presence of a valley to the side of the deformation, similarly to the formation of lateral spreads [91].

The implications of the differences in lithological setting reflect those already known in the literature and give relevant information for landslide hazard assessments, especially since DSGSDs have the potential for violent landslides at a large scale [33,48,49,53]. The investigation of surface features in relation to bedding can indeed provide useful insights for prevention strategies and resilience practices in areas where such geohazards are widespread. For example, repetitive slope strike-parallel surface features on cataclinal slopes might indicate the presence of a complex basal shear zone composed of different strata moving independently, which likely bear a higher failure risk. On the other hand, the presence of surface features parallel to the slope dip might point to a progressive release of tension, with implications on the brittleness and stability of DSGSD landforms.

The recognition of surface features in the identification and classification of DSGSDs could also help other remote surveys on unreachable areas of the Earth and other planetary bodies. Remote identification of key features can be extensively applied to DSGSDs on the basis of a few evident surface markers and provide support in investigations where field activity is unfeasible, time-limited or completely impossible. Considering the recent and possible future limitations to travel for geopolitical or health safety reasons, and the fresh interest for the surface geomorphology of Mars and other planets, moons, and planetoids [92,93], such approach would provide useful comparisons for the complexity of large-scale slope processes in both inner and outer space.

6. Conclusions

The investigation of this area of the northern Apennines allowed the observation of an array of DSGSDs connected to different lithostructural settings. Different patterns of geomorphological features distributed on their surface could be attributed to the effect of bedding and folding. On both cataclinal and anaclinal slopes surface features are similar in nature, but different in occurrence and expression: features parallel to the strike of the slope appear more developed on cataclinal slopes, where bedding seems to favour the gravitational movement downslope. On the case of a DSGSD transversal to a vertical fold hinge, the release of vertical axial fractures produced a corrugated appearance with deep vertical cuts which mask the presence of other features.

Lithostructural control seems not the main contributing factor in the activation of basal shear zones in DSGSDs in sedimentary contexts but can have a significant impact on their further characteristics, evolution, and movement. The complexity of DSGSDs as landforms not only manifests in their polygenetic origin, but above all in the range of processes promoting their evolution after detachment. The variety of surface morphologies produced by different lithostructural constraints can be very high and produce great diversity in the expression of these landforms. In extreme cases, most of the standard features associated to DSGSDs might not even be visible. Efforts in the recognition and characterisation of these forms in the field must take into account these variations in order to provide meaningful

information on the potential geomorphological hazard represented by these landforms, especially when associated with human occupation. In this context, surface features and their investigation on the basis of open source maps and remote sensing data represent a potential source of information about the internal characteristics of DSGSDs, as each of them is produced by a variety of different processes. These observations are useful both for the detection and inventory of potential geohazards, and for the investigations through remote sensing techniques of unreachable areas where precise field data cannot be retrieved.

Author Contributions: Conceptualization, G.S.M. and A.Z.; methodology, G.S.M. and A.Z.; formal analysis, G.S.M.; investigation, G.S.M.; writing—original draft preparation, G.S.M.; writing—review and editing, A.Z.; visualization, G.S.M.; funding acquisition, A.Z. All authors have read and agreed to the published version of the manuscript.

Funding: Part of this research was supported by the Italian Ministry of Education, University, and Research (MIUR) through the project “Dipartimenti di Eccellenza 2018–2022” (WP4–Risorse del Patrimonio Culturale) awarded to the Dipartimento di Scienze della Terra “A. Desio” of the Università degli Studi di Milano. Field survey funded by the SUCCESSO-TERRA Project, financed by the Italian Ministry of Education, University and Research (MIUR), grant PRIN20158KBLNB (P.Is. M. Cremaschi and A. Zerboni). APC partially supported by Università degli Studi di Milano (Fondo di Ateneo per APC); additional financial contribution from the project CTE_NAZPR19AZERB_01 (P.I. A. Zerboni).

Acknowledgments: The authors are thankful to the owners and staff of the “Hotel Sporting” in Febbio (Villa Minozzo, RE) and “Residence Hotel Matilde” in Carpineti (RE) for their hospitality and support during field surveys.

Conflicts of Interest: The authors declare no conflict of interest.

References

1. Dramis, F.; Sorriso-Valvo, M. Deep-seated gravitational slope deformations, related landslides and tectonics. *Eng. Geol.* **1994**, *38*, 231–243. [[CrossRef](#)]
2. Agliardi, F.; Crosta, G.; Zanchi, A. Structural constraints on deep-seated slope deformation kinematics. *Eng. Geol.* **2001**, *59*, 83–102. [[CrossRef](#)]
3. Zischinsky, U. Movement of unstable valley sides. *Ges. Geol. Bergbaustud. Mitteil Ungen* **1966**, *17*, 127–168.
4. Zischinsky, U. Über Sackungen. *Rock Mech.* **1969**, *1*, 30–52. [[CrossRef](#)]
5. Nemcok, A. Classification of landslides and other mass movements. *Rock Mech.* **1972**, *4*, 71–78. [[CrossRef](#)]
6. Radbruch-hall, D.H. Gravitational Creep of Rock Masses on Slopes. In *Developments in Geotechnical Engineering*; Voight, B., Ed.; Elsevier: Amsterdam, The Netherlands, 1978; Volume 14, pp. 607–657.
7. Mahr, T. Deep—Reaching gravitational deformations of high mountain slopes. *Bull. Int. Assoc. Eng. Geol.* **1977**, *16*, 121–127. [[CrossRef](#)]
8. McCalpin, J.; Irvine, J.R. Sackungen at the Aspen Highlands Ski Area, Pitkin County, Colorado. *Environ. Eng. Geosci.* **1995**, *1*, 277–290. [[CrossRef](#)]
9. Bovis, M.J.; Evans, S.G. Extensive deformations of rock slopes in southern Coast Mountains, southwest British Columbia, Canada. *Eng. Geol.* **1996**, *44*, 163–182. [[CrossRef](#)]
10. Evans, S.G.; Couture, R. The 1965 Hope Slide, British Columbia; catastrophic failure of a sagging rock slope. In Proceedings of the Geological Society of America Annual Meeting, Denver, CO, USA, 27–30 October 2002.
11. Soldati, M.; Corsini, A.; Pasuto, A. Landslides and climate change in the Italian Dolomites since the Late glacial. *Catena* **2004**, *55*, 141–161. [[CrossRef](#)]
12. Gutiérrez-Santolalla, F.; Acosta, E.; Ríos, S.; Guerrero, J.; Lucha, P. Geomorphology and geochronology of sacking features (uphill-facing scarps) in the Central Spanish Pyrenees. *Geomorphology* **2005**, *69*, 298–314. [[CrossRef](#)]
13. Taramelli, A.; Melelli, L. Map of deep seated gravitational slope deformations susceptibility in central Italy derived from SRTM DEM and spectral mixing analysis of the Landsat ETM+ data. *Int. J. Remote Sens.* **2008**, *30*, 357–387. [[CrossRef](#)]
14. Audemard, F.; Beck, C.; Carrillo, E. Deep-seated gravitational slope deformations along the active Boconó Fault in the central portion of the Mérida Andes, western Venezuela. *Geomorphology* **2010**, *124*, 164–177. [[CrossRef](#)]

15. Ambrosi, C.; Crosta, G.B. Valley shape influence on deformation mechanisms of rock slopes. *Geol. Soc. Lond. Spéc. Publ.* **2011**, *351*, 215–233. [[CrossRef](#)]
16. Agliardi, F.; Crosta, G.B.; Frattini, P.; Malusà, M.G. Giant non-catastrophic landslides and the long-term exhumation of the European Alps. *Earth Planet. Sci. Lett.* **2013**, *365*, 263–274. [[CrossRef](#)]
17. Chigira, M.; Hariyama, T.; Yamasaki, S. Development of deep-seated gravitational slope deformation on a shale dip-slope: Observations from high-quality drill cores. *Tectonophysics* **2013**, *605*, 104–113. [[CrossRef](#)]
18. Crosta, G.; Frattini, P.; Agliardi, F. Deep seated gravitational slope deformations in the European Alps. *Tectonophysics* **2013**, *605*, 13–33. [[CrossRef](#)]
19. Coquin, J.; Mercier, D.; Bourgeois, O.; Cossart, E.; Decaulne, A. Gravitational spreading of mountain ridges coeval with Late Weichselian deglaciation: Impact on glacial landscapes in Tröllaskagi, northern Iceland. *Quat. Sci. Rev.* **2015**, *107*, 197–213. [[CrossRef](#)]
20. Pánek, T.; Klimeš, J. Temporal behavior of deep-seated gravitational slope deformations: A review. *Earth-Sci. Rev.* **2016**, *156*, 14–38. [[CrossRef](#)]
21. Oppikofer, T.; Saintot, A.; Hermanns, R.; Böhme, M.; Scheiber, T.; Gosse, J.; Dreiås, G. From incipient slope instability through slope deformation to catastrophic failure — Different stages of failure development on the Ivasnasen and Vollan rock slopes (western Norway). *Geomorphology* **2017**, *289*, 96–116. [[CrossRef](#)]
22. Mariani, G.S.; Cremaschi, M.; Zerboni, A.; Zuccoli, L.; Trombino, L. Geomorphology of the Mt. Cusna Ridge (Northern Apennines, Italy): Evolution of a Holocene landscape. *J. Maps* **2018**, *14*, 392–401. [[CrossRef](#)]
23. Frattini, P.; Crosta, G.B.; Rossini, M.; Allievi, J. Activity and kinematic behaviour of deep-seated landslides from PS-InSAR displacement rate measurements. *Landslides* **2018**, *15*, 1053–1070. [[CrossRef](#)]
24. Mège, D.; Bourgeois, O. Equatorial glaciations on Mars revealed by gravitational collapse of Valles Marineris wallslopes. *Earth Planet. Sci. Lett.* **2011**, *310*, 182–191. [[CrossRef](#)]
25. Kromuszczyńska, O.; Mège, D.; Dębniak, K.; Gurgurewicz, J.; Makowska, M.; Lucas, A. Deep-seated gravitational slope deformation scaling on Mars and Earth: Same fate for different initial conditions and structural evolutions. *Earth Surf. Dyn.* **2019**, *7*, 361–376. [[CrossRef](#)]
26. Crosta, G.B.; Frattini, P.; Valbuzzi, E.; De Blasio, F.V. Introducing a New Inventory of Large Martian Landslides. *Earth Space Sci.* **2018**, *5*, 89–119. [[CrossRef](#)]
27. Chigira, M. Long-term gravitational deformation of rocks by mass rock creep. *Eng. Geol.* **1992**, *32*, 157–184. [[CrossRef](#)]
28. Aringoli, D.; Gentili, B.; Materazzi, M.; Pambianchi, G. Mass movements in Adriatic central Italy: Activation and evolutive control factors. In *Landslides: Causes, Types and Effects*; Nova Science Publishers, Inc.: New York, NY, USA, 2010.
29. Crosta, G.B. Landslide, spreading, deep seated gravitational deformation: Analysis, examples, problems and proposals. *Geogr. Fis. E Din. Quat.* **1996**, *19*, 297–313.
30. Ambrosi, C.; Crosta, G. Large sackung along major tectonic features in the Central Italian Alps. *Eng. Geol.* **2006**, *83*, 183–200. [[CrossRef](#)]
31. Jomard, H.; Lebourg, T.; Guglielmi, Y. Morphological analysis of deep-seated gravitational slope deformation (DSGSD) in the western part of the Argentera massif. A morpho-tectonic control? *Landslides* **2013**, *11*, 107–117. [[CrossRef](#)]
32. McCalpin, J.P. Criteria for determining the seismic significance of sackungen and other scarplike landforms in mountainous regions. In *Techniques for Identifying Faults and Determining their Origins*; US Nuclear Regulatory Commission: Washington, DC, USA, 1999; pp. 2–55.
33. Gori, S.; Falcucci, E.; Dramis, F.; Galadini, F.; Galli, P.; Giaccio, B.; Messina, P.; Pizzi, A.; Sposato, A.; Cosentino, D. Deep-seated gravitational slope deformation, large-scale rock failure, and active normal faulting along Mt. Morrone (Sulmona basin, Central Italy): Geomorphological and paleoseismological analyses. *Geomorphology* **2014**, *208*, 88–101. [[CrossRef](#)]
34. Aringoli, D.; Gentili, B.; Pambianchi, G.; Piscitelli, A.M. The contribution of the ‘Sibilla Appenninica’ legend to karst knowledge in the Sibillini Mountains (Central Apennines, Italy). *Geol. Soc. Lond. Spéc. Publ.* **2007**, *273*, 329–340. [[CrossRef](#)]
35. Martinotti, G.; Giordan, D.; Giardino, M.; Ratto, S. Controlling factors for deep-seated gravitational slope deformation (DSGSD) in the Aosta Valley (NW Alps, Italy). *Geol. Soc. Lond. Spéc. Publ.* **2011**, *351*, 113–131. [[CrossRef](#)]
36. Ballantyne, C.K. Paraglacial geomorphology. *Quat. Sci. Rev.* **2002**, *21*, 1935–2017. [[CrossRef](#)]

37. Hippolyte, J.-C.; Bourlès, D.; Leanni, L.; Braucher, R.; Chauvet, F.; Lebatard, A. 10Be ages reveal >12ka of gravitational movement in a major sackung of the Western Alps (France). *Geomorphology* **2012**, *171*, 139–153. [[CrossRef](#)]
38. Aringoli, D.; Gentili, B.; Materazzi, M.; Pambianchi, G.; Sciarra, N. DSGSDs Induced by Post-Glacial Decompression in Central Apennine (Italy). In *Landslide Science and Practice*; Springer Science and Business Media: Berlin, Germany, 2013; pp. 417–423.
39. Pánek, T.; Mentlík, P.; Ditchburn, B.; Zondervan, A.; Norton, K.P.; Hradecký, J. Are sackungen diagnostic features of (de)glaciated mountains? *Geomorphology* **2015**, *248*, 396–410. [[CrossRef](#)]
40. Chigira, M.; Tsou, C.-Y.; Matsushi, Y.; Hiraishi, N.; Matsuzawa, M. Topographic precursors and geological structures of deep-seated catastrophic landslides caused by Typhoon Talas. *Geomorphology* **2013**, *201*, 479–493. [[CrossRef](#)]
41. Tsou, C.-Y.; Chigira, M.; Matsushi, Y.; Chen, S.-C. Deep-seated gravitational deformation of mountain slopes caused by river incision in the Central Range, Taiwan: Spatial distribution and geological characteristics. *Eng. Geol.* **2015**, *196*, 126–138. [[CrossRef](#)]
42. Kinakin, D.; Stead, D. Analysis of the distributions of stress in natural ridge forms: Implications for the deformation mechanisms of rock slopes and the formation of sackung. *Geomorphology* **2005**, *65*, 85–100. [[CrossRef](#)]
43. Hippolyte, J.-C.; Brocard, G.; Tardy, M.; Nicoud, G.; Bourlès, D.; Braucher, R.; Menard, G.; Souffaché, B. The recent fault scarps of the Western Alps (France): Tectonic surface ruptures or gravitational sackung scarps? A combined mapping, geomorphic, levelling, and 10Be dating approach. *Tectonophysics* **2006**, *418*, 255–276. [[CrossRef](#)]
44. Agliardi, F.; Zanchi, A.; Crosta, G.B. Tectonic vs. gravitational morphostructures in the central Eastern Alps (Italy): Constraints on the recent evolution of the mountain range. *Tectonophysics* **2009**, *474*, 250–270. [[CrossRef](#)]
45. Jibson, R.W.; Harp, E.L.; Schulz, W.; Keefer, D.K. Landslides Triggered by the 2002 Denali Fault, Alaska, Earthquake and the Inferred Nature of the Strong Shaking. *Earthq. Spectra* **2004**, *20*, 669–691. [[CrossRef](#)]
46. Moro, M.; Saroli, M.; Salvi, S.; Stramondo, S.; Doumaz, F. The relationship between seismic deformation and deep-seated gravitational movements during the 1997 Umbria–Marche (Central Italy) earthquakes. *Geomorphology* **2007**, *89*, 297–307. [[CrossRef](#)]
47. Chigira, M.; Kiho, K. Deep-seated rockslide-avalanches preceded by mass rock creep of sedimentary rocks in the Akaishi Mountains, central Japan. *Eng. Geol.* **1994**, *38*, 221–230. [[CrossRef](#)]
48. Crosta, G.; Chen, H.; Frattini, P. Forecasting hazard scenarios and implications for the evaluation of countermeasure efficiency for large debris avalanches. *Eng. Geol.* **2006**, *83*, 236–253. [[CrossRef](#)]
49. Chigira, M. September 2005 rain-induced catastrophic rockslides on slopes affected by deep-seated gravitational deformations, Kyushu, southern Japan. *Eng. Geol.* **2009**, *108*, 1–15. [[CrossRef](#)]
50. Moro, M.; Saroli, M.; Gori, S.; Falcucci, E.; Galadini, F.; Messina, P. The interaction between active normal faulting and large scale gravitational mass movements revealed by paleoseismological techniques: A case study from central Italy. *Geomorphology* **2012**, *151*, 164–174. [[CrossRef](#)]
51. Pedrazzini, A.; Jaboyedoff, M.; Loye, A.; Derron, M.-H. From deep seated slope deformation to rock avalanche: Destabilization and transportation models of the Sierre landslide (Switzerland). *Tectonophysics* **2013**, *605*, 149–168. [[CrossRef](#)]
52. Zangerl, C.; Eberhardt, E.; Perzmaier, S. Kinematic behaviour and velocity characteristics of a complex deep-seated crystalline rockslide system in relation to its interaction with a dam reservoir. *Eng. Geol.* **2010**, *112*, 53–67. [[CrossRef](#)]
53. Paronuzzi, P.; Rigo, E.; Bolla, A. Influence of filling–drawdown cycles of the Vajont reservoir on Mt. Toc slope stability. *Geomorphology* **2013**, *191*, 75–93. [[CrossRef](#)]
54. Stead, D.; Wolter, A. A critical review of rock slope failure mechanisms: The importance of structural geology. *J. Struct. Geol.* **2015**, *74*, 1–23. [[CrossRef](#)]
55. Varnes, D.J. Slope movement types and processes. In *Landslides, Analysis and Control*; Special Report; Transportation and Road Research Board, National Academy of Sciences: Washington, DC, USA, 1978; pp. 11–33.
56. Guzzetti, F.; Cardinali, M.; Reichenbach, P. The Influence of Structural Setting and Lithology on Landslide Type and Pattern. *Environ. Eng. Geosci.* **1996**, *II*, 531–555. [[CrossRef](#)]

57. Břežný, M.; Pánek, T.; Lenart, J.; Grygar, R.; Tábořík, P.; McColl, S.T. Sackung and enigmatic mass movement folds on a structurally-controlled mountain ridge. *Geomorphology* **2018**, *322*, 175–187. [[CrossRef](#)]
58. Massironi, M.; Genevois, R.; Floris, M.; Stefani, M. Influence of the antiformal setting on the kinematics of a large mass movement: The Passo Vallaccia, eastern Italian Alps. *Bull. Int. Assoc. Eng. Geol.* **2010**, *70*, 497–506. [[CrossRef](#)]
59. Bistacchi, A.; Massironi, M.; Superchi, L.; Zorzi, L.; Francese, R.; Giorgi, M.; Chistolini, F.; Genevois, R. A 3D geological model of the 1963 Vajont landslide. *Ital. J. Eng. Geol. Environ.* **2013**, *6*, 531–539.
60. Hou, Y.; Chigira, M.; Tsou, C.-Y. Numerical study on deep-seated gravitational slope deformation in a shale-dominated dip slope due to river incision. *Eng. Geol.* **2014**, *179*, 59–75. [[CrossRef](#)]
61. Chalupa, V.; Pánek, T.; Tábořík, P.; Klimeš, J.; Hartvich, F.; Grygar, R. Deep-seated gravitational slope deformations controlled by the structure of flysch nappe outliers: Insights from large-scale electrical resistivity tomography survey and LiDAR mapping. *Geomorphology* **2018**, *321*, 174–187. [[CrossRef](#)]
62. Aringoli, D.; Gentili, B.; Materazzi, M.; Pambianchi, G. Deep-seated gravitational slope deformations in active tectonics areas of the Umbria-Marche Apennine (Central Italy). *Geogr. Fis. Dinam. Quat.* **2010**, *33*, 127–140.
63. Aringoli, D.; Gentili, B.; Pambianchi, G. The role of recent tectonics in controlling the deep-seated gravitational deformation of Mount Frascare (central Apennines). *Geogr. Fis. Dinam. Quat.* **1996**, *19*, 281–286.
64. Trigila, A.; Iadanza, C. *Landslides in Italy*; Italian National Institute for Environmental Protection and Research (ISPRA): Roma, Italy, 2008.
65. Vai, F.; Martini, I.P. *Anatomy of an Orogen: The Apennines and Adjacent Mediterranean Basins*; Springer: Berlin, Germany, 2013.
66. Bosellini, A. *Storia Geologica d'Italia: Gli ultimi 200 milioni di anni*; Zanichelli: Bologna, Italy, 2005.
67. Zoetemeijer, R.; Sassi, W.; Roure, F.; Cloetingh, S. Stratigraphic and kinematic modeling of thrust evolution, northern Apennines, Italy. *Geology* **1992**, *20*, 1035. [[CrossRef](#)]
68. Finetti, I.; Boccaletti, M.; Bonini, M.; Del Ben, A.; Geletti, R.; Pipan, M.; Sani, F. Crustal section based on CROP seismic data across the North Tyrrhenian–Northern Apennines–Adriatic Sea. *Tectonophysics* **2001**, *343*, 135–163. [[CrossRef](#)]
69. Pini, G.A. *Tectonosomes and Olistostromes in the Argille Scagliose of the Northern Apennines, Italy*; Geological Society of America: Boulder, CO, USA, 1999; Volume 335.
70. Livani, M.; Scrocca, D.; Arecco, P.; Doglioni, C. Structural and Stratigraphic Control on Salient and Recess Development Along a Thrust Belt Front: The Northern Apennines (Po Plain, Italy). *J. Geophys. Res. Solid Earth* **2018**, *123*, 4360–4387. [[CrossRef](#)]
71. Gelati, R. *Storia geologica del paese Italia*; Diabasis: Parma, Italy, 2013.
72. Pellegrini, L.; Vercesi, P.L. Landscapes and Landforms Driven by Geological Structures in the Northwestern Apennines. In *World Geomorphological Landscapes*; Springer Science and Business Media: Berlin, Germany, 2017; pp. 203–213.
73. Bertolini, G.; Corsini, A.; Tellini, C. Fingerprints of Large-Scale Landslides in the Landscape of the Emilia Apennines. In *World Geomorphological Landscapes*; Springer Science and Business Media: Berlin, Germany, 2017; pp. 215–224.
74. Bertolini, G.; Canuti, P.; Casagli, N.; De Nardo, M.T.; Egidi, D.; Mainetti, M.; Pignone, R.; Pizziolo, M. *Carta della Pericolosità Relativa da Frana della Regione Emilia-Romagna*; SystemCart: Rome, Italy, 2002.
75. Regione Emilia-Romagna Carta Inventario delle frane e Archivio storico delle frane. Available online: <https://ambiente.regione.emilia-romagna.it/it/geologia/cartografia/webgis-banchedati/cartografia-dissesto-idrogeologico> (accessed on 29 June 2020).
76. Carlini, M.; Chelli, A.; Vescovi, P.; Artoni, A.; Clemenzi, L.; Tellini, C.; Torelli, L. Tectonic control on the development and distribution of large landslides in the Northern Apennines (Italy). *Geomorphology* **2016**, *253*, 425–437. [[CrossRef](#)]
77. Bertolini, G. Radiocarbon Dating on Landslides in the Northern Apennines (Italy). In *Landslides and Climate Change: Challenges and Solutions*; Mathie, E., McInnes, R., Fairbank, H., Jakeways, J., Eds.; Taylor & Francis: London, UK, 2007; pp. 73–80.
78. Bertolini, G.; Tellini, C. New radiocarbon dating for landslide occurrences in the Emilia Apennines (Northern Italy). *Trans. Jpn. Geomorphol. Union* **2001**, *22*, C-23.

79. Compostella, C.; Mariani, G.S.; Trombino, L. Holocene environmental history at the treeline in the Northern Apennines, Italy: A micromorphological approach. *Holocene* **2014**, *24*, 393–404. [[CrossRef](#)]
80. Bertolini, G.; Pellegrini, M. The landslides of Emilia Apennines (northern Italy) with reference to those which resumed activity in the 1994–1999 period and required Civil Protection interventions. *Quad. Geol.* **2001**, *8*, 27–74.
81. Mariani, G.S.; Brandolini, F.; Pelfini, M.; Zerboni, A. Matilda’s castles, northern Apennines: Geological and geomorphological constrains. *J. Maps* **2019**, *15*, 521–529. [[CrossRef](#)]
82. Mariani, G.S.; Compostella, C.; Trombino, L. Complex climate-induced changes in soil development as markers for the Little Ice Age in the Northern Apennines (Italy). *Catena* **2019**, *181*, 104074. [[CrossRef](#)]
83. Losacco, U. La glaciazione quaternaria dell’Appennino settentrionale. *Riv. Geogr. Ital.* **1949**, *56*, 90–152.
84. Losacco, U. Gli antichi ghiacciai dell’Appennino settentrionale: Studio morfologico e paleogeografico. *Atti Soc. Nat. Mat. Modena* **1982**, *113*, 1–24.
85. Morelli, S.; Pazzi, V.; Frodella, W.; Fanti, R. Kinematic Reconstruction of a Deep-Seated Gravitational Slope Deformation by Geomorphic Analyses. *Geosciences* **2018**, *8*, 26. [[CrossRef](#)]
86. Regione Emilia-Romagna Cartografia di Base. Available online: <https://geoportale.regione.emilia-romagna.it/catalogo/dati-cartografici/cartografia-di-base> (accessed on 29 June 2020).
87. Regione Emilia-Romagna Banca Dati Geologica, 1:10.000. Available online: <https://geoportale.regione.emilia-romagna.it/catalogo/dati-cartografici/informazioni-geoscientifiche/geologia/banca-dati-geologica-1-10.000> (accessed on 29 June 2020).
88. Jaboyedoff, M.; Penna, I.; Pedrazzini, A.; Baroň, I.; Crosta, G.B. An introductory review on gravitational-deformation induced structures, fabrics and modeling. *Tectonophysics* **2013**, *605*, 1–12. [[CrossRef](#)]
89. Papani, G.; De Nardo, M.T.; Bettelli, G.; Rio, D.; Tellini, C.; Vernia, L. *Note Illustrative della Carta Geologica d’Italia alla Scala 1:50.000, Foglio 218 Castelnuovo ne’ Monti*; Servizio Geologico d’Italia: Regione Emilia Romagna, Italy, 2002.
90. Savage, W.Z.; Varnes, D.J. Mechanics of gravitational spreading of steep-sided ridges («sackung»). *Bull. Int. Assoc. Eng. Geol.* **1987**, *35*, 31–36. [[CrossRef](#)]
91. Carobene, L.; Cevasco, A. A large scale lateral spreading, its genesis and Quaternary evolution in the coastal sector between Cogoleto and Varazze (Liguria—Italy). *Geomorphology* **2011**, *129*, 398–411. [[CrossRef](#)]
92. Baker, V.R. Planetary landscape systems: A limitless frontier. *Earth Surf. Process. Landf.* **2008**, *33*, 1341–1353. [[CrossRef](#)]
93. Baker, V.R. The modern evolution of geomorphology—Binghamton and personal perspectives, 1970–2019 and beyond. *Geomorphology* **2019**, 106684. [[CrossRef](#)]



© 2020 by the authors. Licensee MDPI, Basel, Switzerland. This article is an open access article distributed under the terms and conditions of the Creative Commons Attribution (CC BY) license (<http://creativecommons.org/licenses/by/4.0/>).